Some remarks about the experiements on neutron, LCP, residues, excitation functions, and pion measurements

Detlef Filges and Frank Goldenbaum

Institut für Kernphysik

Forschungszentrum Jülich GmbH

Germany

15. Oktober 2009

IAEA Benchnark Excercise, 6-7 Oct., 2009, Vienna, Austria

LANL experiments at the WNR Los Alamos

(W. B. Amian et al., Nucl. Sci. Eng. 112 (1992) 78,

M. Meier et al., Nucl. Sci. Eng. 110 (1993) 289)

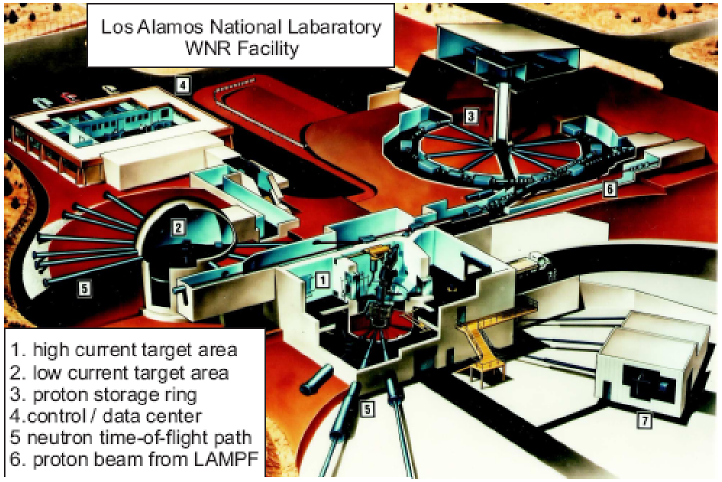

An artist's view of the WNR facility

The beam structure at LAMPF and at WNR

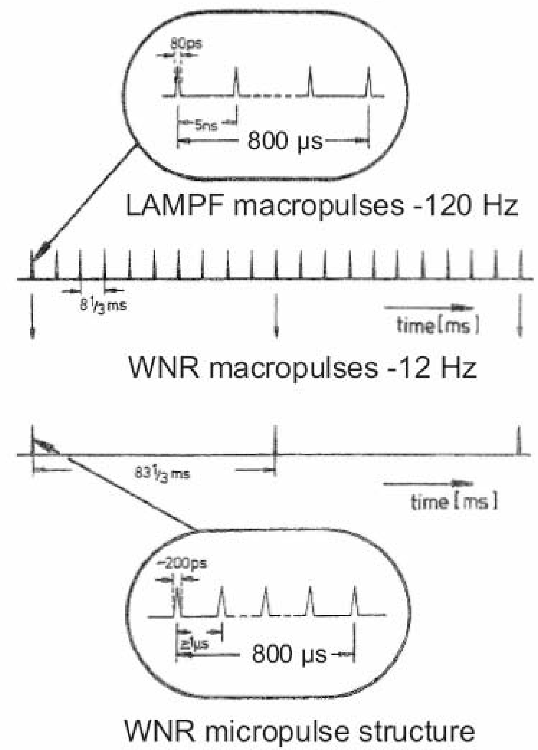

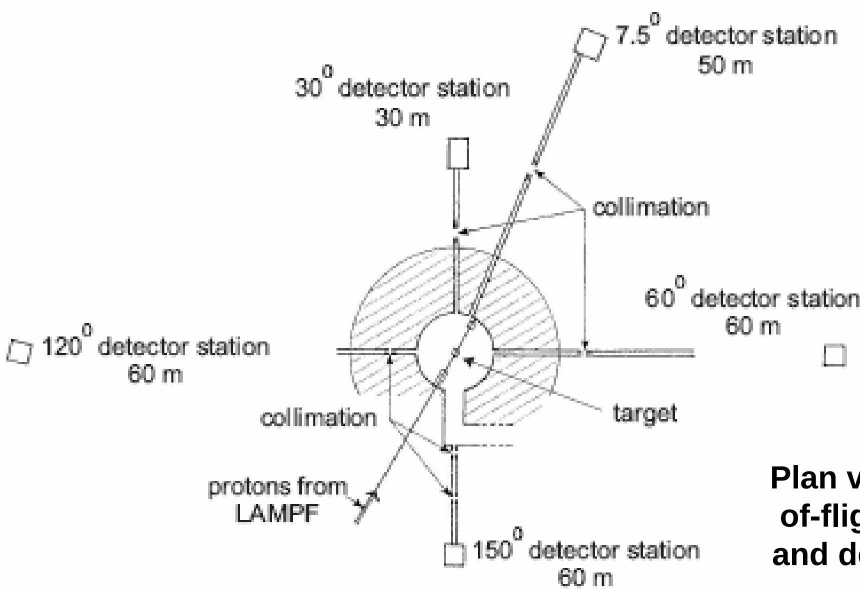

Plan view of the time-of-flight lines, target and detector stations

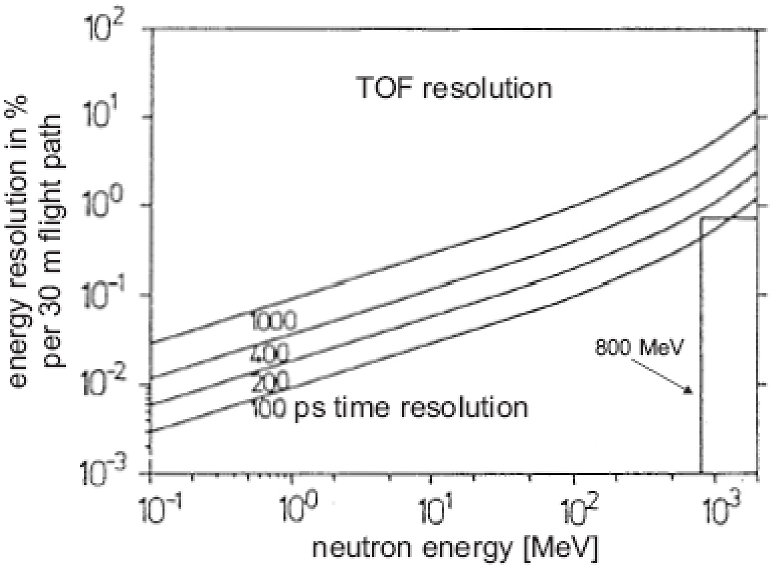

Neutron energy resolution for a 30 m flight path length

Experimental uncertainties for protons of 0.597 GeV (Amian/Meier et al.)

correction	magnitude	uncertainty in %
time dependent background	< 0.01	< 5
target-produced background	< 0.05	20
shadowbar-background	< 0.08	< 3
air transmission	> 0.45	< 2.5
uranium transmission < 20MeV	> 0.32	5
uranium transmission > 20MeV	> 042	< 20
detector efficiency	0.03 to 0.20	5 to 20
live time	> 071	< 5
charge normalization	1.0	5

Detectors and experiments of Stamer and Scobel et al.

flight path	7.5^0	30^0	60^0	120^0	150^0
flight path length [m]	50.36	29.76	58.61	23.34	30.99
material	BC-501	NE-213	BC-501	BC-501	BC-501
dimension					
diameter × thickness [cm]	25.4 × 5.1	10.2 × 10.2	30.5 × 20.3	25.4 × 5.1	30.5 × 20.3
energy / time resolution					
at 256 MeV	16 MeV	16 MeV	15 MeV	29 MeV	26 MeV
incident protons	5.8 ns	53 ns	6.5 ns	4.9 ns	5.9 ns
energy / time resolution					
at 800 MeV	22 MeV	36 MeV	49 MeV	164 MeV	72 MeV
incident protons	1.1 ns	1.0 ns	2.7 ns	3.6 ns	2.1 ns

Target materials used for the different thin target experiments

597 and 800 MeV incident protons (Amian et al. [129, 130])									
target material	Be	BeO	B	BN	C	Al	Fe	Pb	^{238}U
thickness [g cm^{-2}]	1.18	0.85	1.00	0.86	0.56	1.29	1.56	0.89	0.78
256 and 800 MeV incident protons (Stamer, Scobel et al. [131])									
target material	^{7}Li	^{27}Al	^{nat}Zr	^{nat}Pb					
thickness [mg cm^{-2}]	thin metallic foils 70-150								

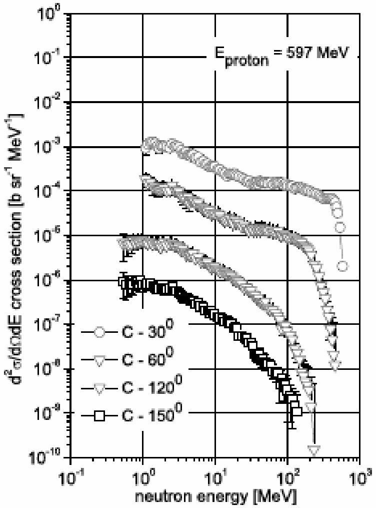

(a) reaction proton (597 MeV) + C target

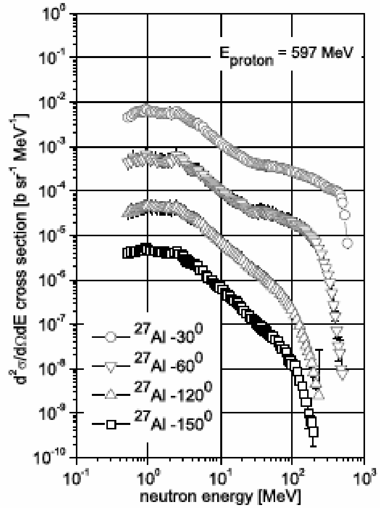

(b) reaction proton (597 MeV) + Al target

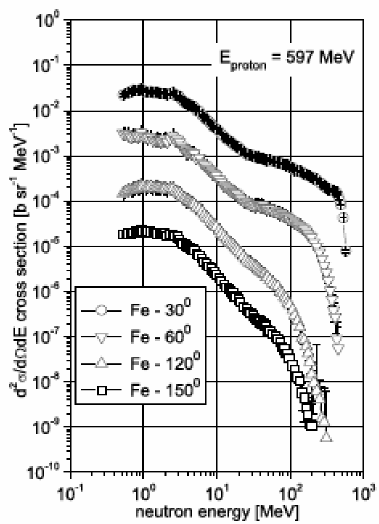

(c) reaction proton (597 MeV) + Fe target

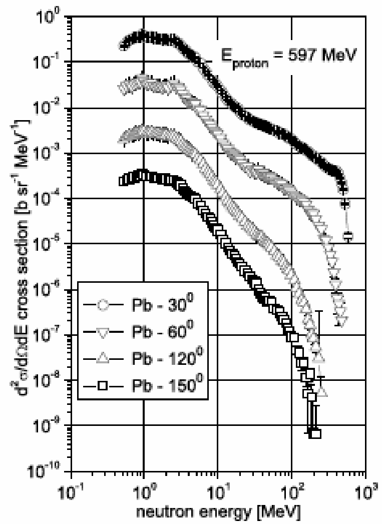

(d) reaction proton (597 MeV) + Pb target

Fig. 10.9 Proton induced experimental double differential neutron production cross sections at scattering angles of $30^0, 60^0, 120^0$, and 150^0 - measurements of Amian et al. [129, 130]. Each successive curve, starting from the smallest angle 30^0, is scaled by a multiplication factor of 10^{-1}, e.g. $60^0 x 10^{-1}$, $120^0 x 10^{-2}$, and $150^0 x 10^{-3}$.

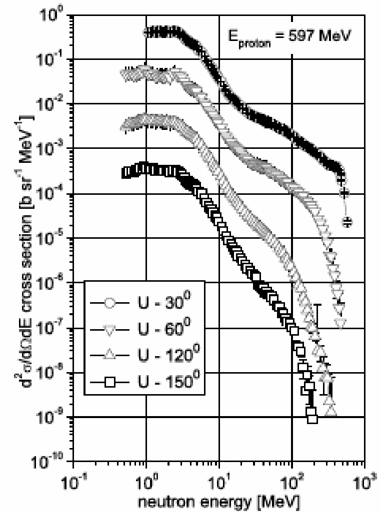

(a) reaction proton (597 MeV) + U target

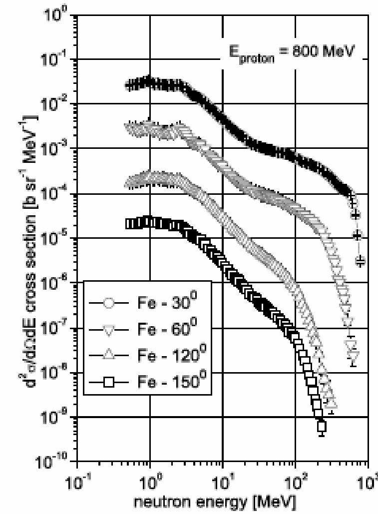

(b) reaction proton (800 MeV) + Fe target

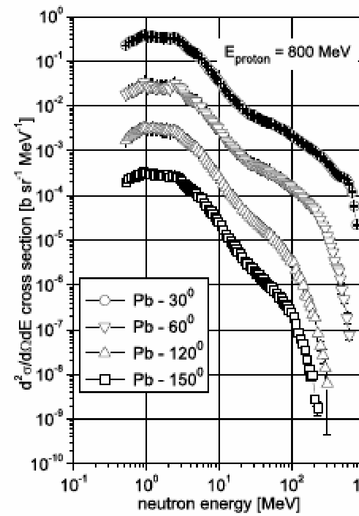

(c) reaction proton (800 MeV) + Pb target

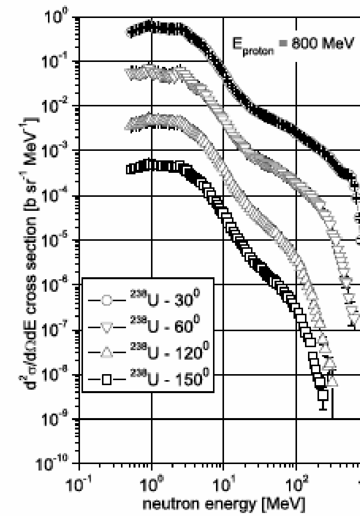

(d) reaction proton (800 MeV) + U target

Fig. 10.10 Proton induced experimental double differential neutron production cross sections at scattering angles of $30^0, 60^0, 120^0$, and 150^0 - measurements of Amian et al. [129, 130]. Each successive curve, starting from the smallest angle 30^0, is scaled by a multiplication factor of 10^{-1}, e.g. $60^0 x 10^{-1}$, $120^0 x 10^{-2}$, and $150^0 x 10^{-3}$.

The SATURNE experiments on double differential neutron cross sections

(S. Leray et al., Phys. Rev. C 65 (2002) 044621)

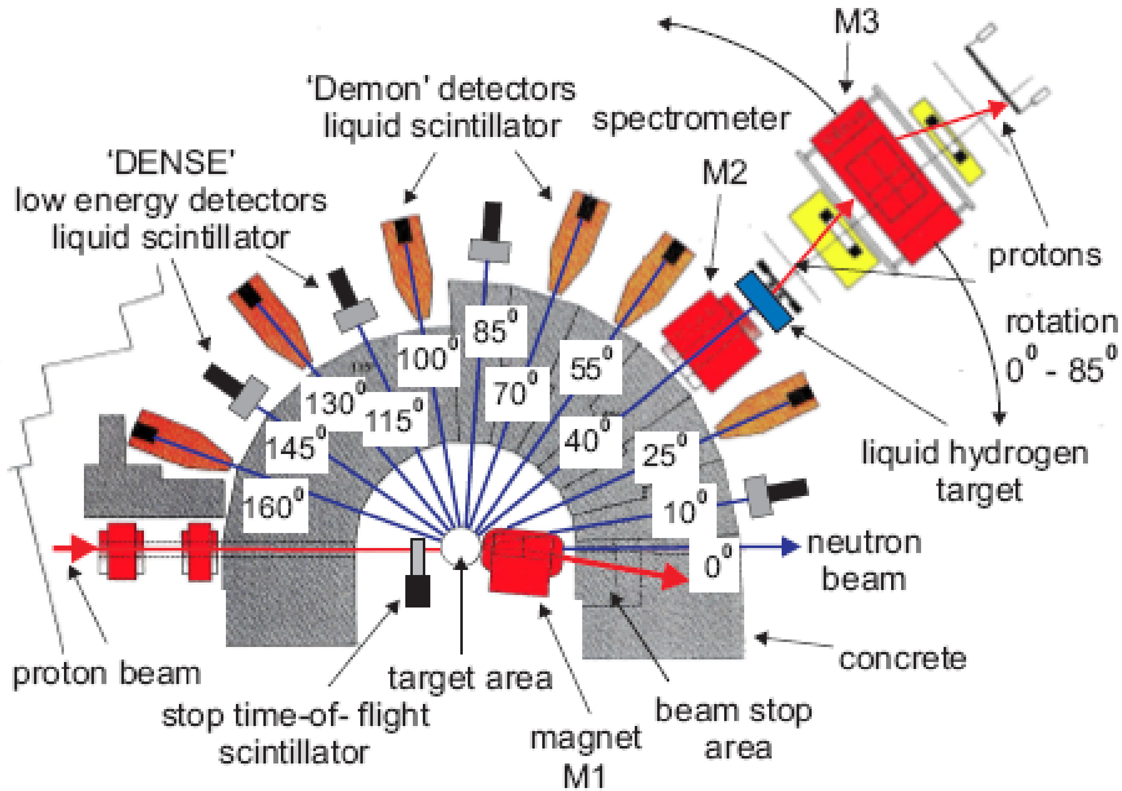

The experimental apparatus of SATURNE, Borne et al., Martinez et.al., and Leray et al.

Detector charateristics

characteristics	DENSE detector	DEMON detector
liquid scintillator	NE-213	NE-213
diameter	127 mm	160 mm
length	51 mm	200
photomultiplier	9390 KB	XP 4512
detector threshold	1.0 MeV	1.9 MeV

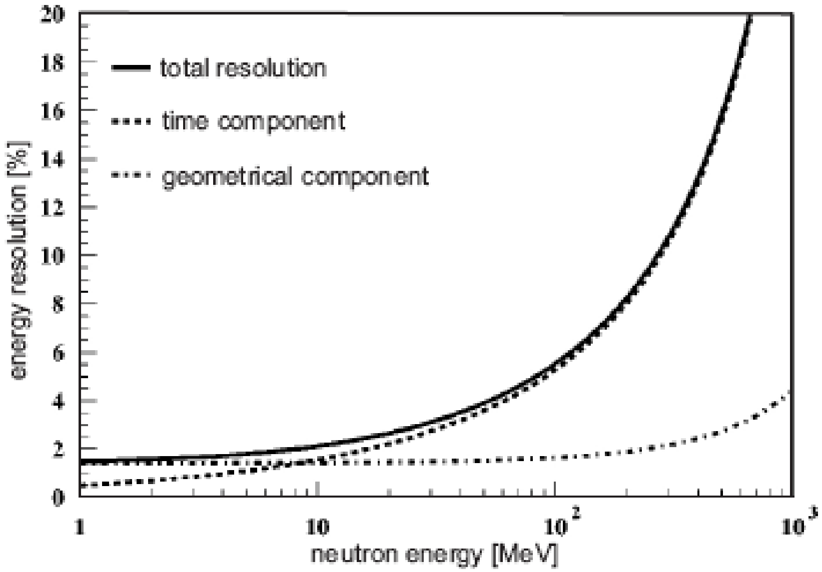

Energy resolution as a function of neutron energy (flight path length = 8.5 m ± 0.06 m).

Time resolution uncertainty is 1.5 ns

Main systemic errors on neutron measurments above proton beam energies ≥ 0.4 GeV (Leray et al.)

error of	incident beam energy [GeV] 0.8 *and* 1.2	1.6
beam intensity	≲ 5.8 %	≲ 5.8 %
spectrometer	≲ 4.0 %	≲ 11.5 %
response function		
unfolding procedure and analysis	≲ 5.8 %	≲ 8.6 %
total uncertainty	≲ 9.1 %	≲ 15.5 %

incident proton energies [GeV]	0.8, 1.2, 1.6					
scattering angles [degree]	0, 10, 25, 40, 55, 85, 100, 115, 130, 145, 160					
target material	Al	Fe	Zr	W	Pb	Th
target thickness [g cm^{-2}]	8.1	23.6	19.4	19.3	22.7	39.8
target diameter [cm]	3.0	3.0	3.0	3.0	3.0	3.0

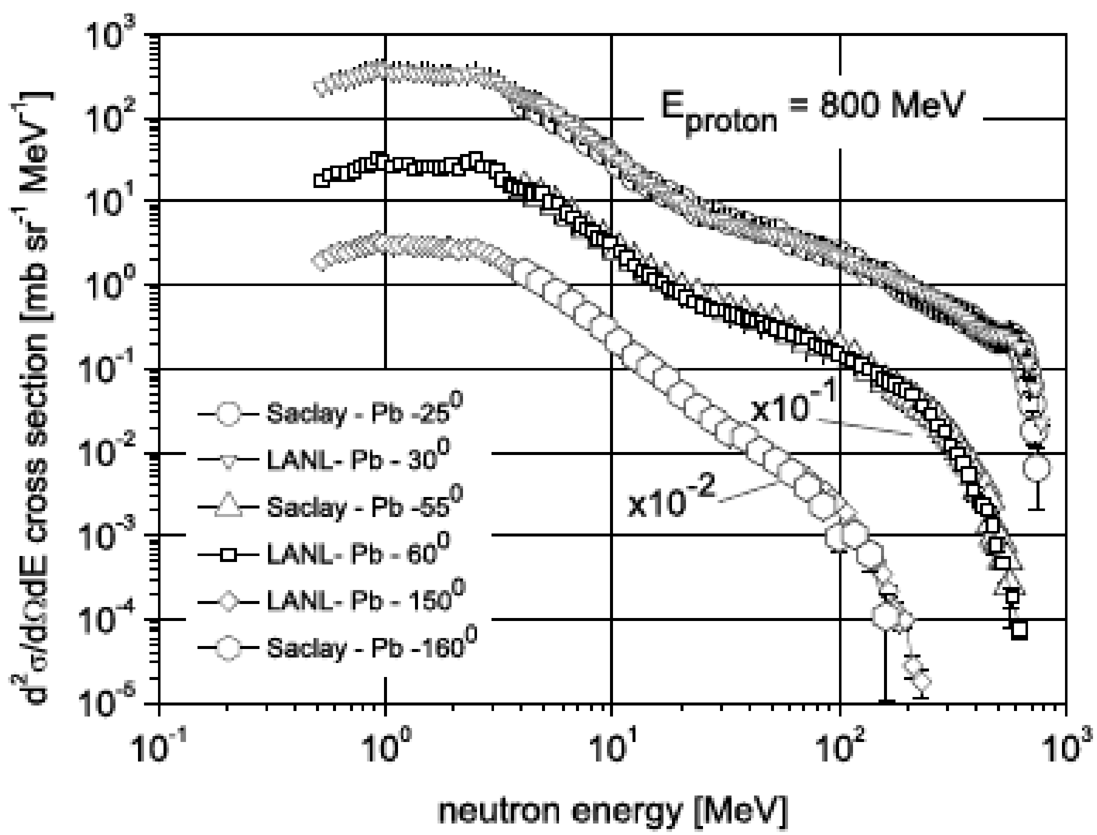

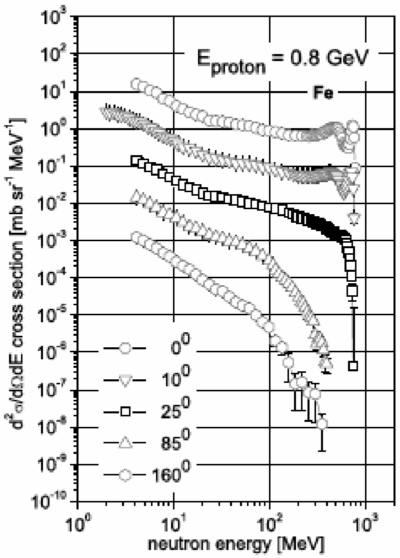

(a) reaction proton (0.8 GeV) + Fe target

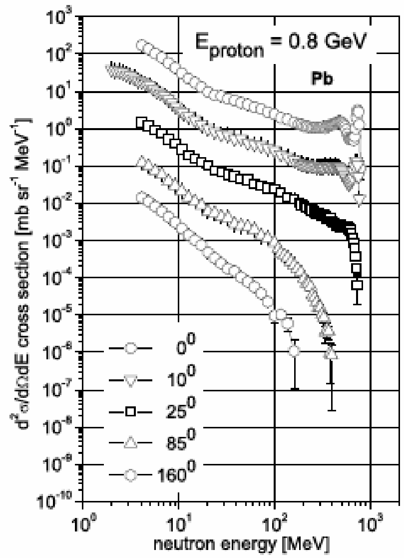

(b) reaction proton (0.8 GeV GeV) + Pb target

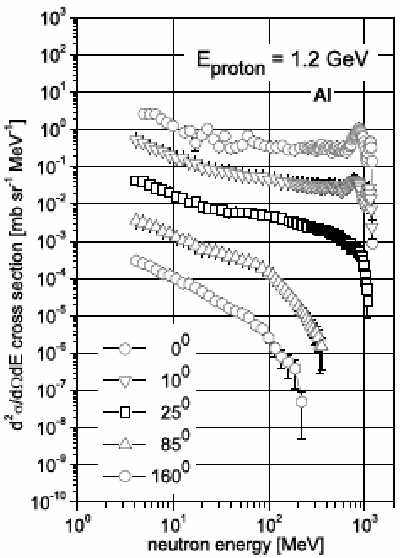

(c) reaction proton (1.2 GeV) + Al target

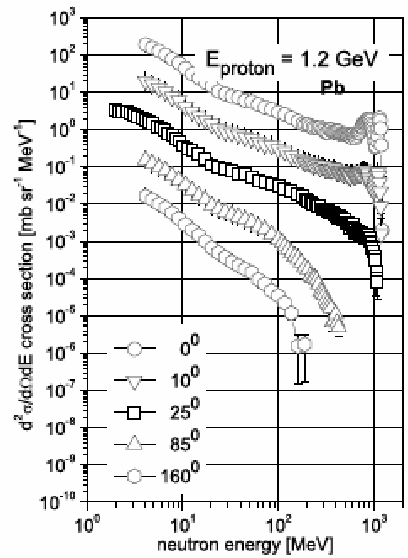

(d) reaction proton (1.2 GeV) + Pb target

Fig. 10.20 Proton induced experimental double differential neutron production cross sections at scattering angles of 0^0,10^0, 25^0, 85^0, and 160^0 - measurements of Ledoux et al. [220] and Leray et al. [132]. Each successive curve, starting from the smallest angle 0^0, is scaled by a multiplication factor of 10^{-1}, e.g. $10^0 x 10^{-1}$, $25^0 x 10^{-2}$, $85^0 x 10^{-3}$, and $160^0 x 10^{-4}$.

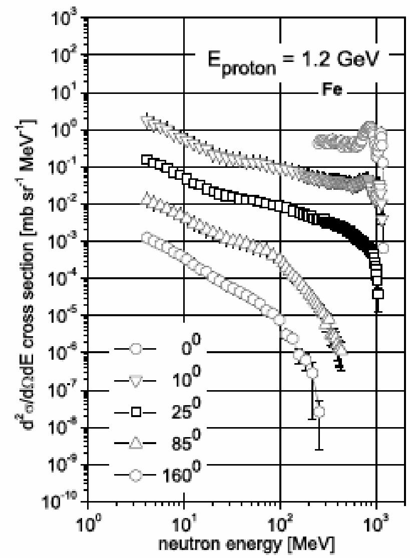

(a) reaction proton (1.2 GeV) + Fe target

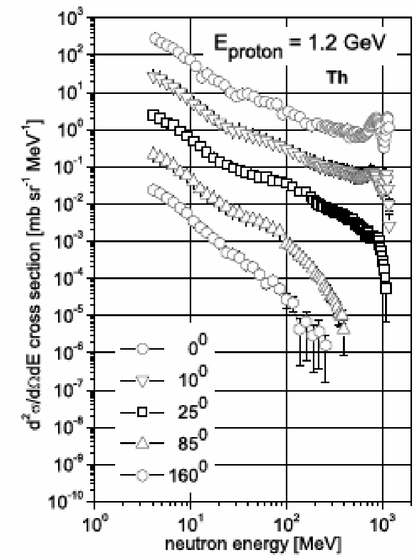

(b) reaction proton (1.2 GeV) +Th target

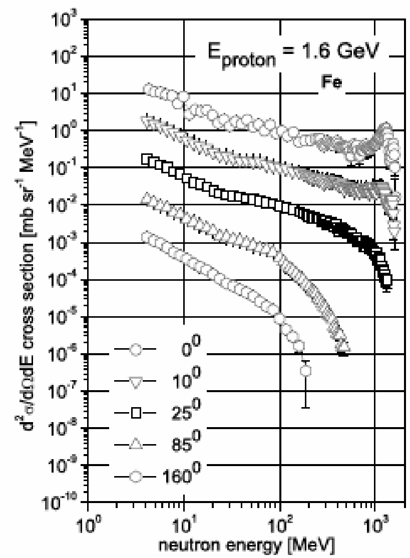

(c) reaction proton (1.6 GeV) + Fe target

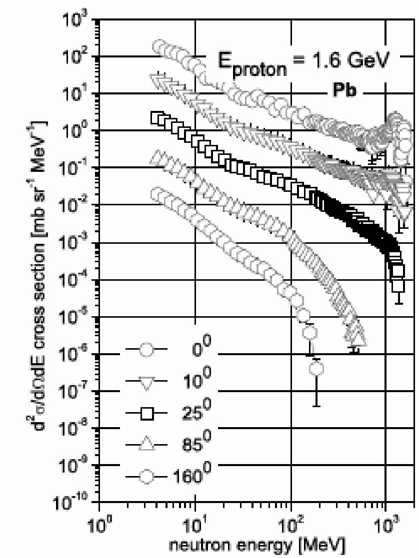

(d) reaction proton (1.6 GeV) + Pb target

Fig. 10.21 The sam as Fig. 10.20.

The KEK neutron double differential measurements

(K. Ishibashi et al., J. of Nucl. Sci. Tech. 34 (1997) 529)

The KEK time-of-flight experimental arrangement (Ishibashi et al.)

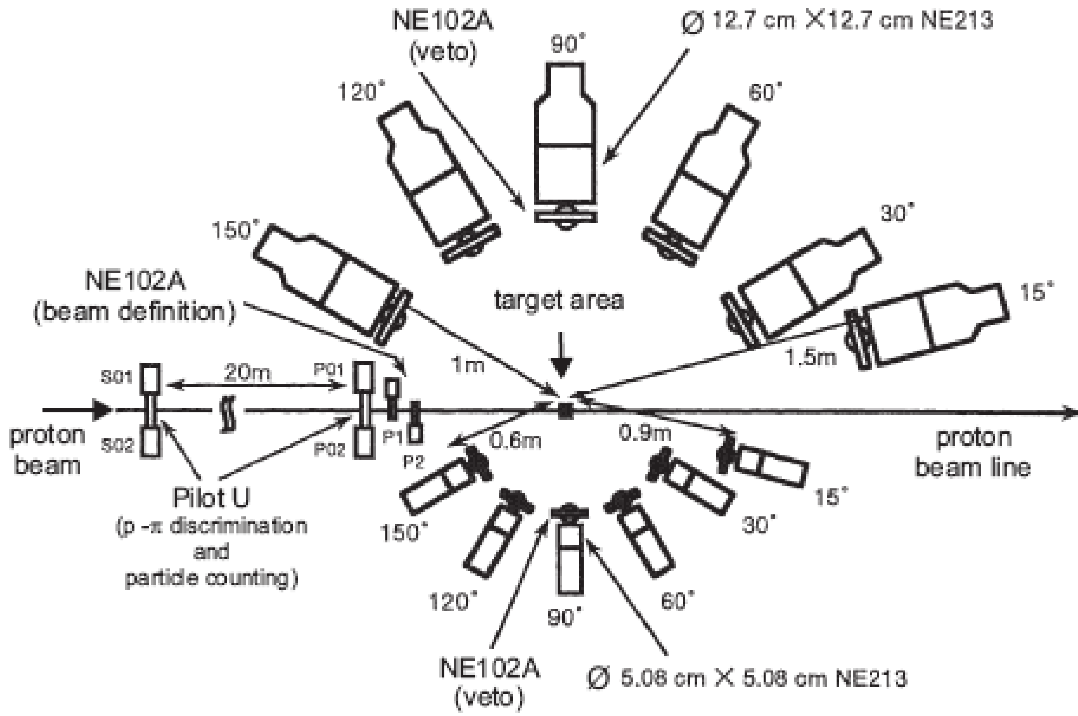

Detector data

flight path	$15^0, 30^0, 60^0, 90^0, 120^0, 150^0$	$15^0, 30^0, 60^0, 90^0, 120^0, 150^0$
flight path length [m]	1.5 - 1.0	0.9 - 0.6
detector material (liquid)	NE-213	NE-213
dimension		
diameter × thickness [cm]	12.7 × 12.7 (5″×5″)	5.08 × 5.08 (2″×2″)
time resolution [ns]	0.5-1.0	
energy resolution $\pm 1\sigma$ [%]	5.7 for 10 MeV neutrons 14.0 for 300 MeV neutrons	

target material	C	Al	Fe	Fe (1.5 GeV)	In	Pb (plate)
diameter [cm]	5.0	5.0	4.9	4.9	4.9	10×10×1.2 cm^3
thickness [g cm^{-2}]	17.5	10.7	23.6	15.74	17.76	13.6
density [g cm^{-3}]	1.75	2.69	7.87	7.87	7.31	11.34
proton energy loss [MeV]:						
at energy 0.8 GeV	37	20	40	-	26	18
at energy 1.5 GeV	33	18	-	24	23	16
at energy 3.0 GeV	33	18	36	-	23	16
mean excitation energy[a] [eV]	73.8	160	278	278	483	819

Target characteristics

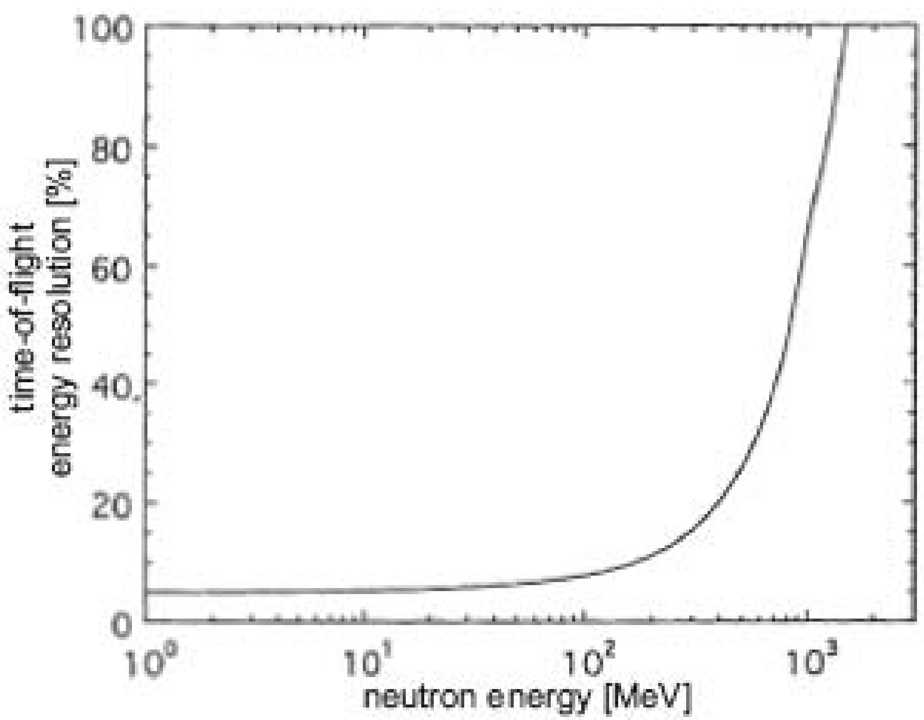

Resulting energy resolution

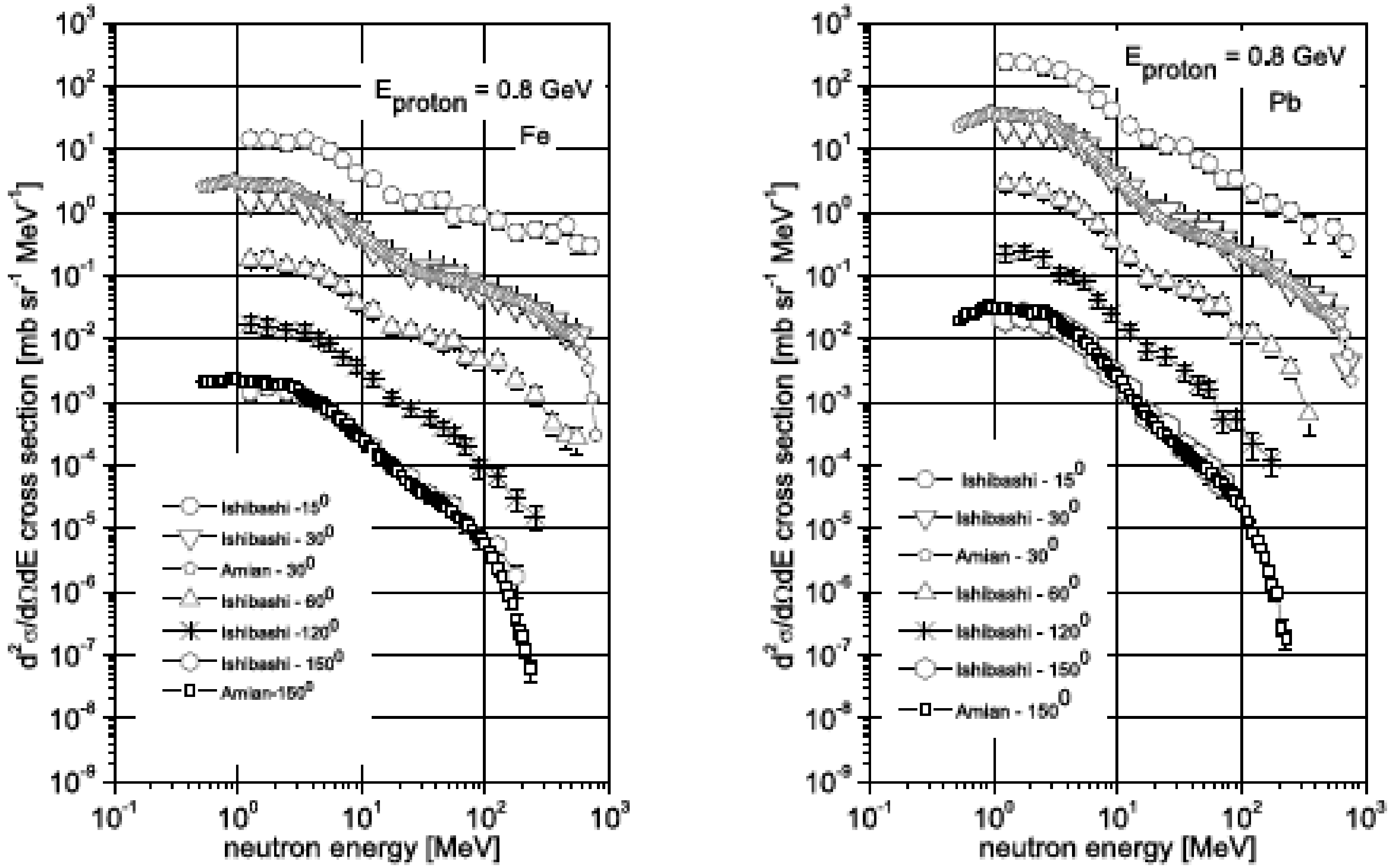

(a) reaction proton (0.8 GeV) + Fe target (b) reaction proton (0.8 GeV) + Pb target

Fig. 10.25 Proton 0.8 GeV induced experimental double differential neutron production cross sections on Fe and Pb targets at scattering angles of 15^0,30^0, 60^0, and 150^0 - measurements of Ishibashi et al. [265] in comparison with measurement of Amian et al. [129] of angles at 30^0 and 150^0. Each successive curve, starting from the smallest angle 15^0, is scaled by a multiplication factor of 10^{-1}, e.g. $30^0 x10^{-1}$, $60^0 x10^{-2}$, $120^0 x10^{-3}$, and $150^0 x10^{-4}$.

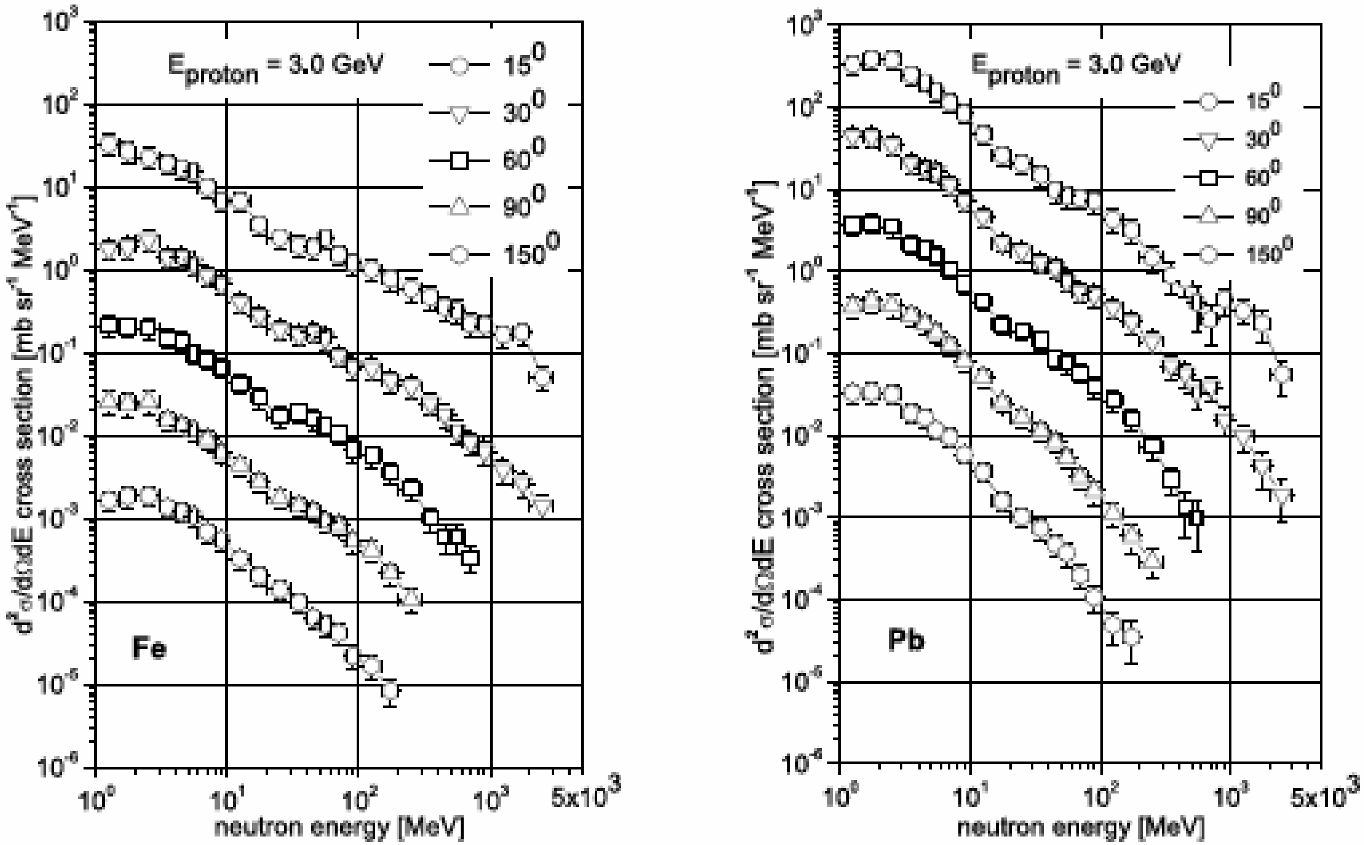

(a) reaction proton (3.0 GeV) + Fe target (b) reaction proton (3.0 GeV) + Pb target

Fig. 10.26 Proton 3.0 GeV induced experimental double differential neutron production cross sections on Fe and Pb targets at scattering angles of 15^0,30^0, 60^0, 90^0, and 150^0 - measurements of Ishibashi et al. [265]. Each successive curve, starting from the smallest angle 15^0, is scaled by a multiplication factor of 10^{-1}, e.g. $30^0 x10^{-1}$, $60^0 x10^{-2}$, $90^0 x10^{-3}$, and $150^0 x10^{-4}$

Multiplicity distributions at COSY and SATURNE

(A. Letourneau et al., Nucl. Inst. Meth. B 170 (2000) 299,

C.-M. Herbach et al., Jülich annual report (2001),

S. Leray et al., Phys. Rev. C 65 (2002) 044621)

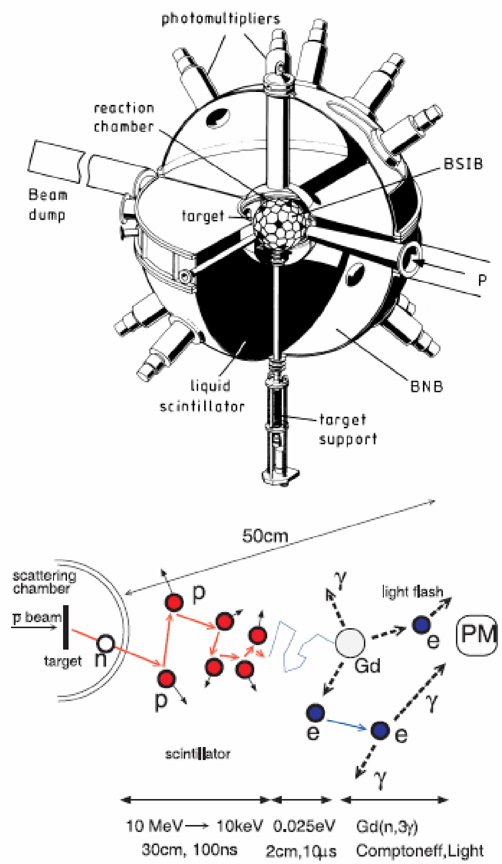

Fig. 10.41 Upper panel (a): Schematic drawing of the NESSI detector system BNB (Berlin Neutron Ball) and the BSiB (Berlin Silicon Ball) in the reaction chamber. Lower panel (b): The principle of neutron detection in the BNB in three steps: i)slowing down/thermalization ii) storage iii) capture, counting.

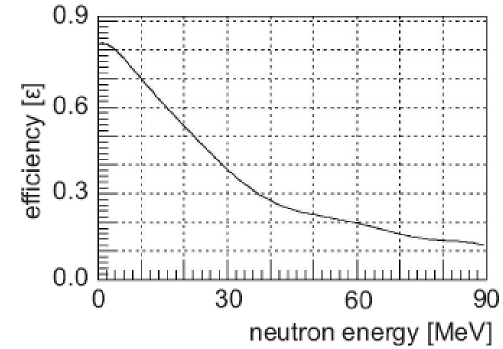

Fig. 10.42 Detection efficiency ε of the BNB as a function of neutron kinetic energy E^n_{kin}, as calculated with the DENIS code [737]. A parameterization of this curve is given in Ref. [115] and Eq. 10.3.

The 4π sr BNB

manufacturer	Hahn-Meitner-Institut Berlin
volume	1.5 m^3
	140 cm
diameter of reaction chamber	40 cm
scintillator liquid	NE343 (1,2,4-trimethylbenzol) C_9H_{12}
gadolinium Gd	0.4% (weight percent)
σ capture[a] for ^{155}Gd and ^{157}Gd	6.1 × 104 and 25.4 × 104 b
number of photo-multipliers	24
energy resolution	no
time resolution[b]	≤ 3 ns
lower trigger threshold	2 MeVee (electron equivalent)

a) Capture cross section for thermal neutrons
b) relative to start-detector

The 4π sr Silicon Ball

	individual silicon detectors
manufacturer	Eurisys Meßtechnik[a]
type	IPH750-500 HMI C
detector-type	surface depletion layer
'backing'	ceramics
active area	763 mm^2
total thickness(depletion zone)	500 μm
spec. resistance	14285 Ωcm
applied voltage	~100 V
max. field strength depl. zone	~3.2 kV/cm
energy res. (5.5 MeV α-source)	<100 keV
time res. (5.5 MeV α-source)	<250 ps

	4π sr silicon ball BSiB
granularity	162 detectors, self-supporting
shape	12 penta-, 90 (ir)regular hexagons
acceptance	91% of 4π sr
radius	10 cm
weight	600 g

Measured (symbols) and calculated (histograms) neutron multiplicity

1.2 GeV p + Al….U

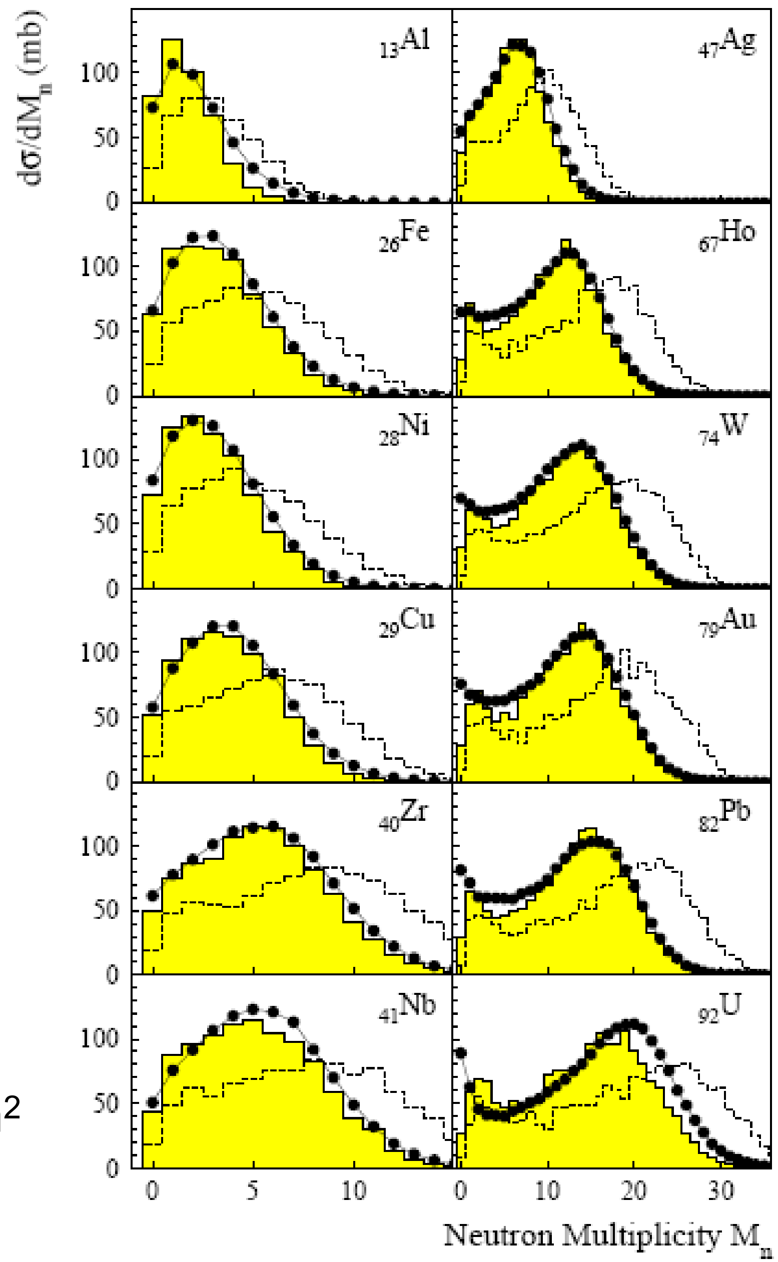

Target thickness 0.1 -1 g/cm²

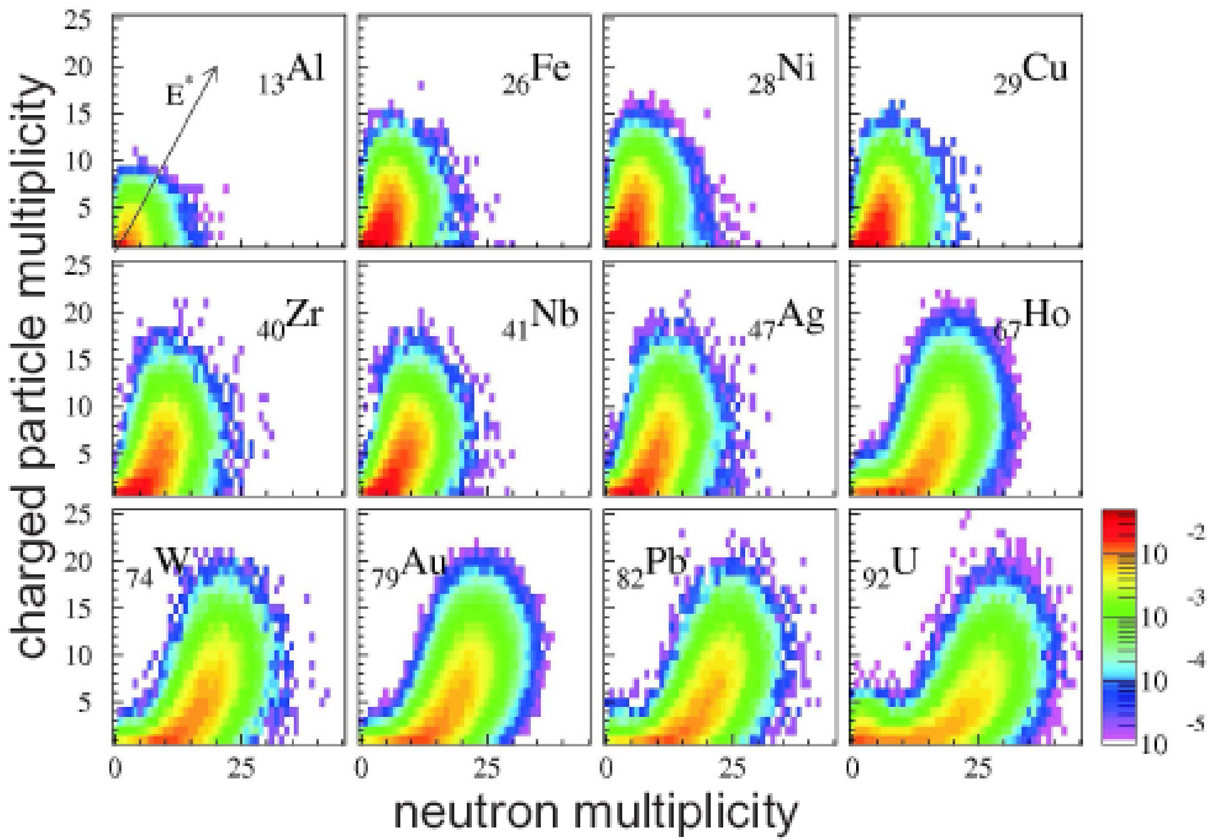

Correlation of measured light charged particle (LCP‘s) versus neutron multiplicity for 2.5 GeV incident protons

-color scale gives the relative yield per multiplicity bin

- the thermal excitation is indicated by the arrow E*

LCP experiments at COSY, LANL, iTHEMBA, and PSI

(R. Chrien et al., Phys. Rev. C 21 (1980) 1014,

J.A. McGill et al., Phys. Rev. C 29 (1984) 204,

J. Franz et al., Nucl. Phys. A 510 (1990) 774,

F. Goldenbaum et al., (unpublished),

S.V. Förtsch et al., Phys. Rev. C 43 (1991) 691,

A. Cowley et al., Phys. Rev. C 54 (1996) 778,

A. Letourneau et al., Nucl. Phys. A 712 (2002) 133,

C.-M. Herbach et al., Nucl. Phys. A 765 (2006) 426,

A. Bubak et al., Phys. Rev. C 76 (2007) 014618,

A. Budzanowski et al., Phys. Rev. C 78 (2008) 024603)

LCP measurements

- **COSY**

  incident proton energies 175 upto 2500 MeV

- **LANL**

  incident proton energies 62 MeV and 800 MeV

- **iTHEMBA**

  incident proton energy 160 MeV

- **PSI**

  incident proton energy 542 MeV

Various total and angle dependent LCPC‘s were measured as

p, d, t, ^{3,4,6}He (and also Li, Be, B c, N, and O isotopes)

PISA experiment

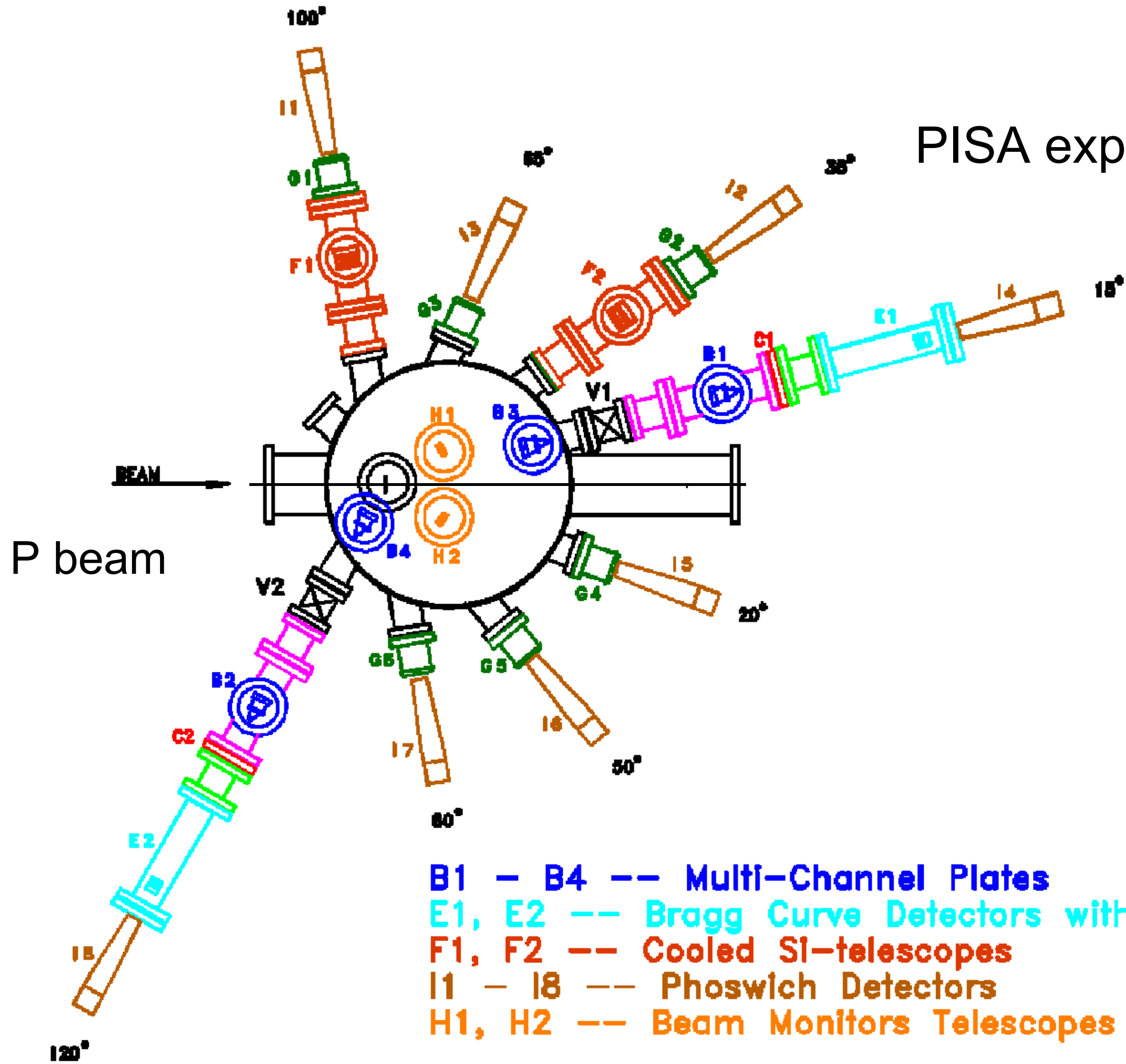

B1 – B4 -- Multi-Channel Plates
E1, E2 -- Bragg Curve Detectors with Si-detectors
F1, F2 -- Cooled Si-telescopes
I1 – I8 -- Phoswich Detectors
H1, H2 -- Beam Monitors Telescopes

V1, V2 -- COSY Valves
C1, C2 -- High Vacuum Protecting Foils

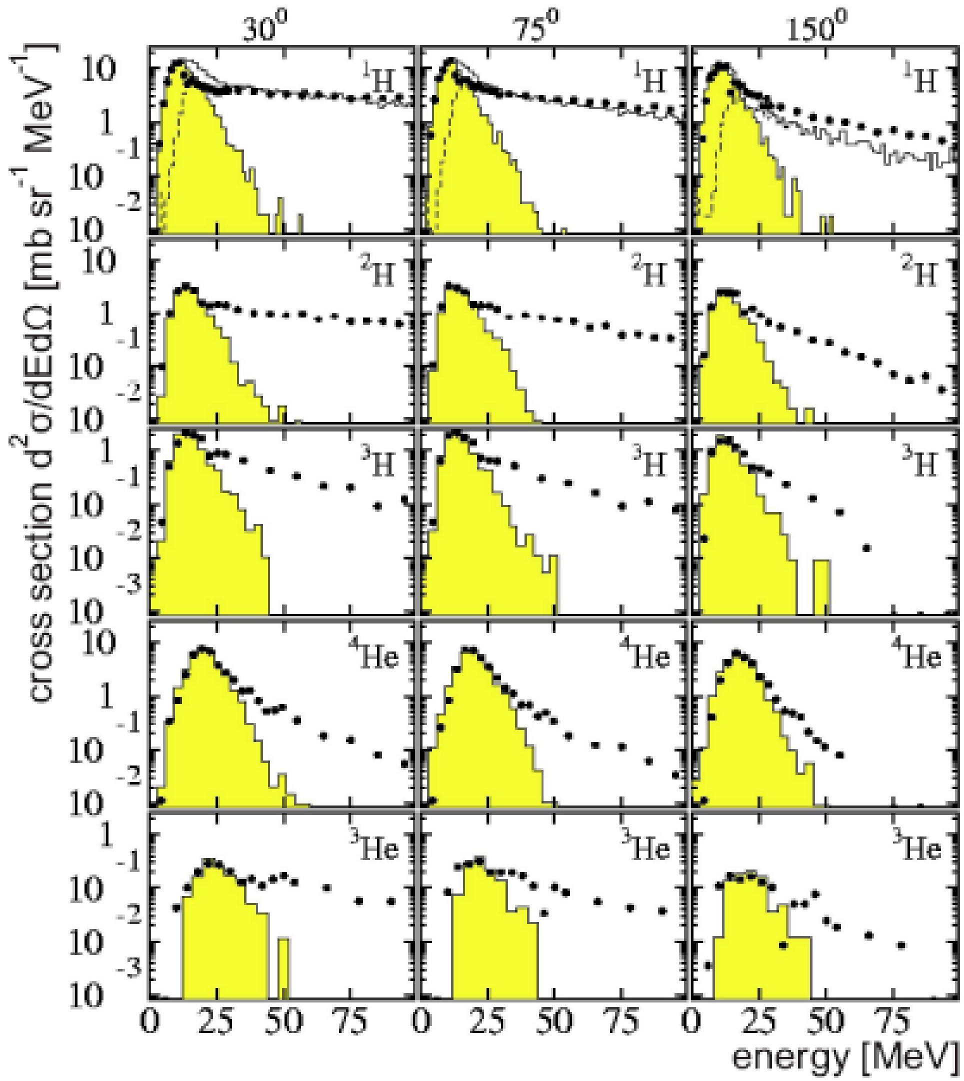

Example of ¹²·³H and ³·⁴He energy spectra for 1.2 GeV p + Ta

(Herbach et al. (2006))

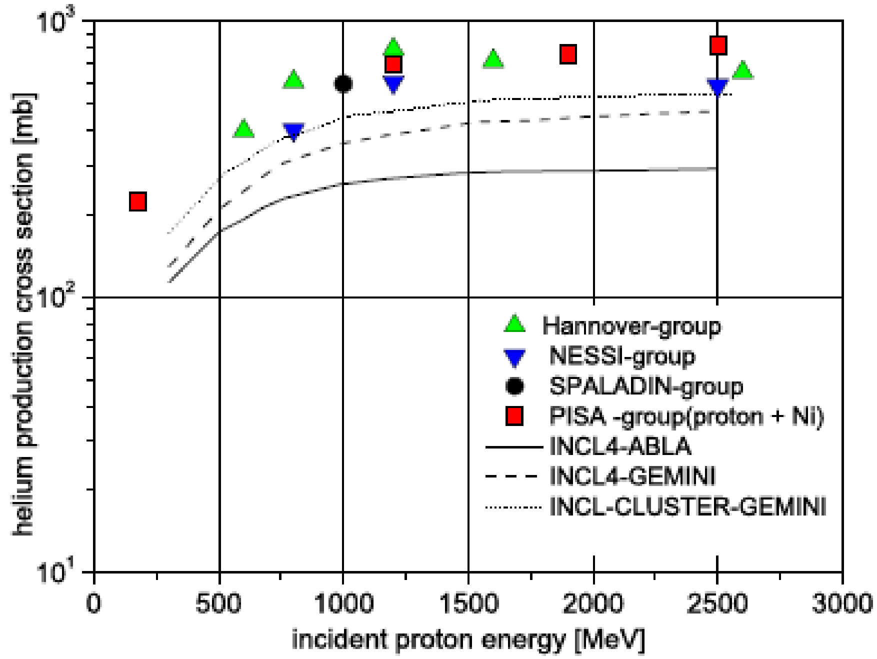

Production cross sections of ^{3,4,6}He isotopes in Fe targets

Isotopic distributions at GSI via inverse kinetic experiments and excitation functions at PSI, ITEP and others

(many publications e.g.:
T. Enqvist et al., Nucl. Phys. A686 (2001) 481,
P. Napolitani et al., Phys. Rev. C 70 (2004) 054607,
L. Audouin et al., Nucl. Phys. A768 (2006) 1,
C. Villagrasa-Canton et al., Phys. Rev. C 75 (2007) 044603, and etc.

M. Gloris et al., Nucl. Instr. and Meth. A463 (2001) 593,
K. Ammon, I. Leya et al., Nucl. Instr. and Meth. B 266 (2008) 2,
Y. E. Titarenko et al., Phys. Rev. C 78 (2008) 034615, and etc.)

Main data base on threshold spallation reaction from Michel and co-workers

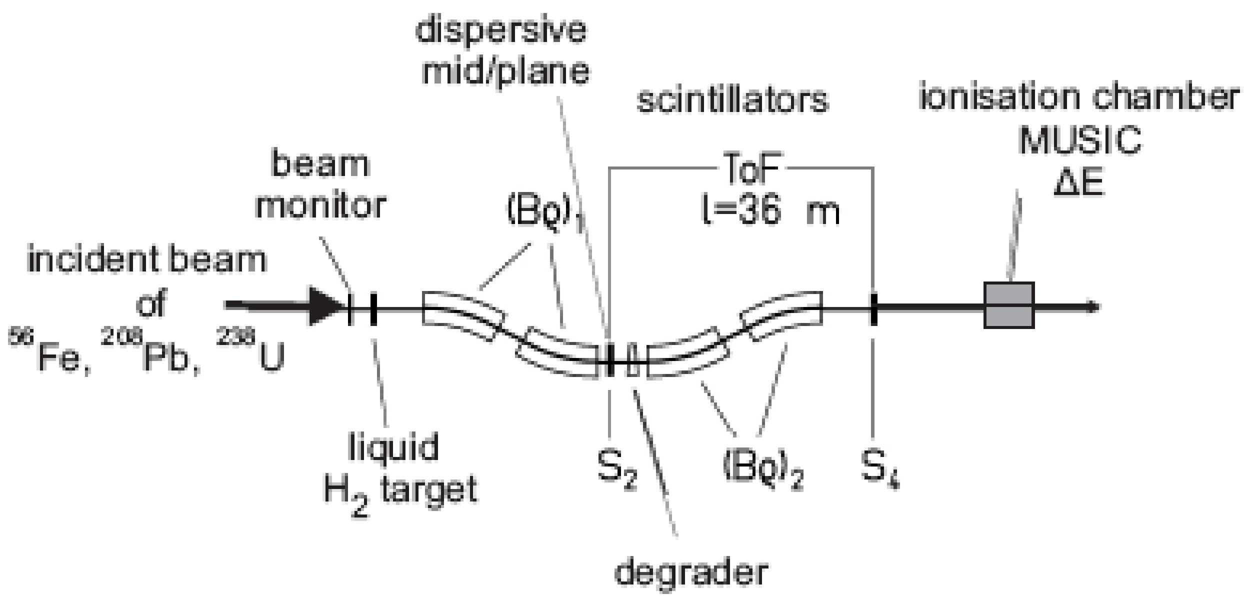

Schematics of the GSI fragment separator FRS

(with the detector arrangement)

Chart of nuclides of residual nuclide
cross sections- reaction Pb-208 + proton

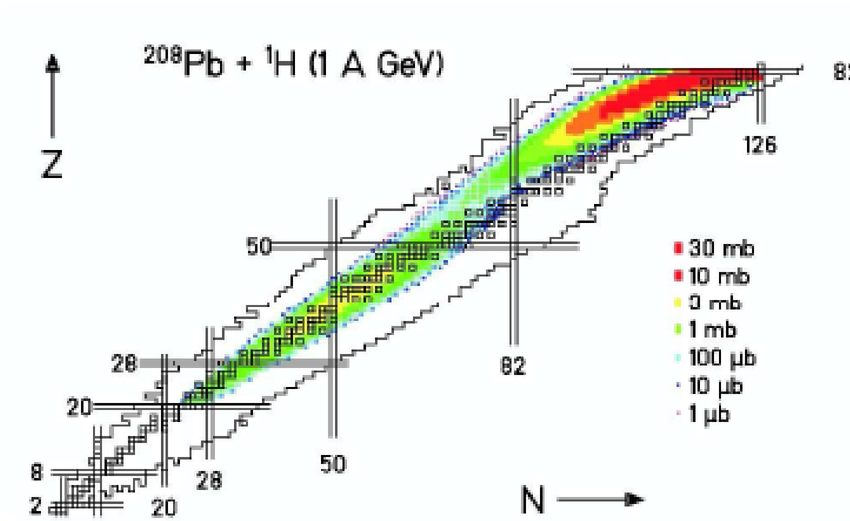

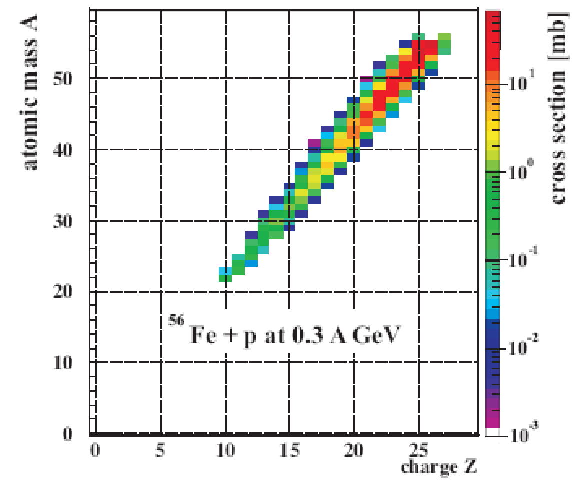

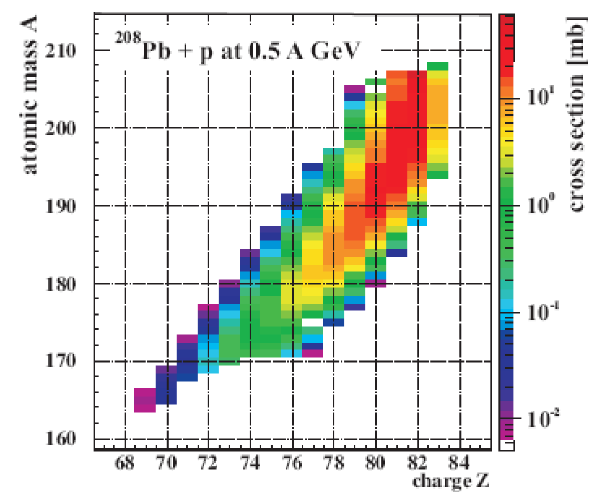

Isotopic cross sections in A-Z projection

Fe-56 + p at 0.4 A GeV

Pb-208 + p at 0.5 A GeV

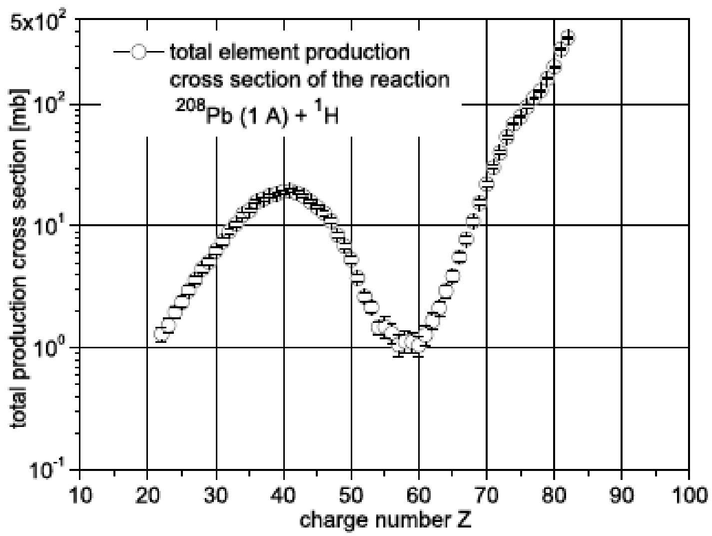

Spallation evaporation
and fission isotopes in Z,

Pb-208(1AGeV) +1H

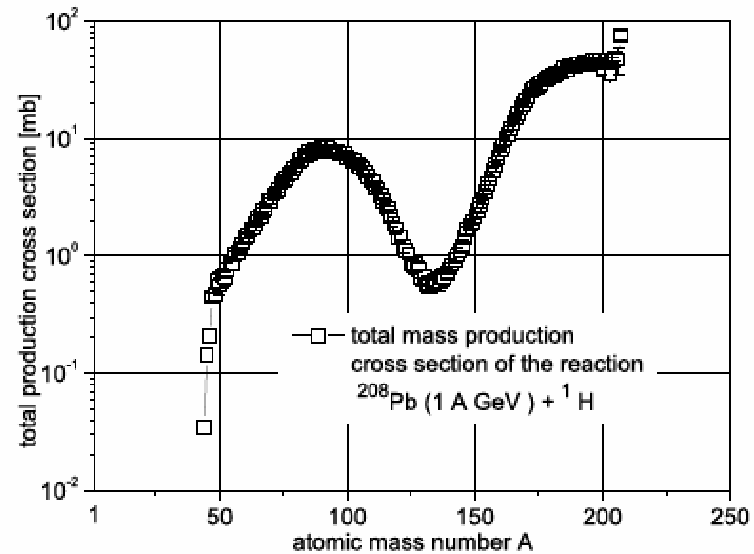

Spallation evaporation
and fission isotopes in A,

Pb-208(1AGeV) +1H

(Data are from Enquist et al.)

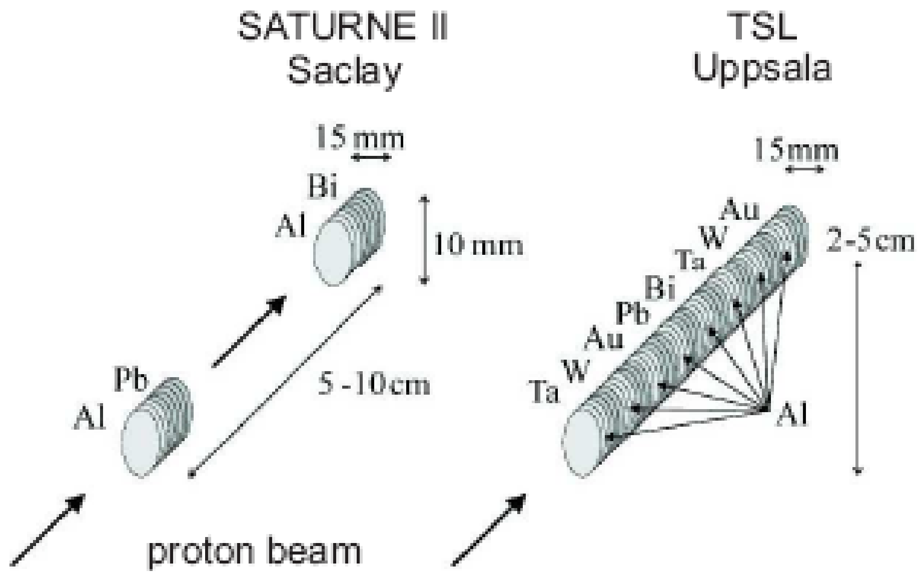

Example of typical foil stacks to measure threshold spallation reactions (Gloris et al. 2001)

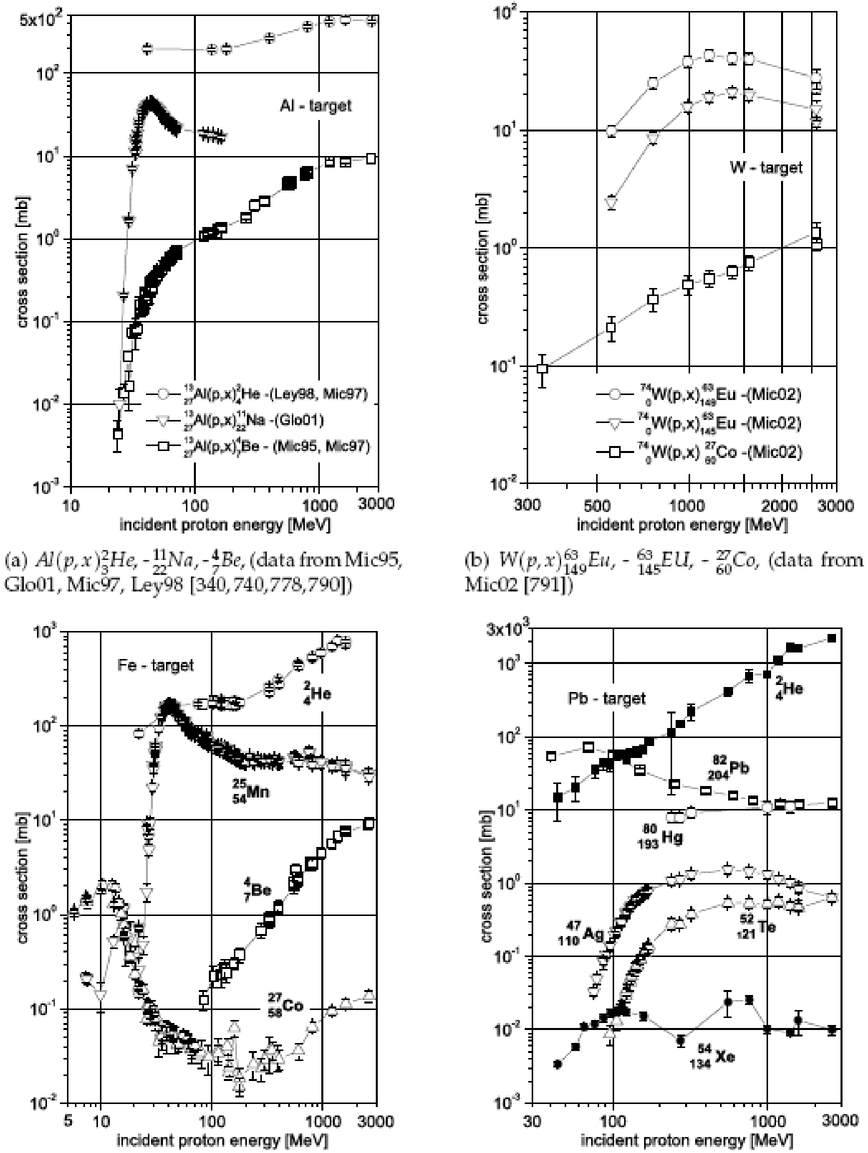

(a) $Al(p,x)^2_3He$, $-^{11}_{22}Na$, $-^4_7Be$, (data from Mic95, Glo01, Mic97, Ley98 [340, 740, 778, 790])

(b) $W(p,x)^{63}_{149}Eu$, $-\ ^{63}_{145}EU$, $-\ ^{27}_{60}Co$, (data from Mic02 [791])

(c) reactions $Fe(p,x)^2_4He$, $-^4_7Be$, $-^{25}_{54}Mn$, $-^{27}_{58}Co$

(d) reactions $Pb(p,x)^2_4He$, $-\ ^{47}_{110}Ag$, $-\ ^{52}_{121}Te$, $-\ ^{54}_{134}Xe$, $-\ ^{80}_{193}Hg$, $-\ ^{82}_{204}Pb$

Fig. 10.64 Excitation functions of residual isotope production of protons on Al, Fe, W, and Pb targets. The cross section data of the lower panels are from: (c) for (^2_4He) from [780], for (^4_7Be) from [791], and for ($^{25}_{54}Mn$, $^{27}_{58}Co$) from [340, 740, 777], and (d) from (^2_4He, $^{54}_{134}Xe$) from [741], for ($^{47}_{110}Ag$, $^{52}_{121}Te$, $^{80}_{193}Hg$) from [778], and for ($^{82}_{204}Pb$) from [781].

Pion double differential measurements at Berkley, PSI and KEK

(D. R. F. Cochran et al., Phys. Rev. D 6 (1972) 3085,

J. F. Crawford et al., Helvetica Physica Acta 53 (1980) 597,

J. F. Crawford et al., Phys. Rev. C22, (1980) 1184,

H. En'yo et al., Phys. Lett. 159B (1985) 1)

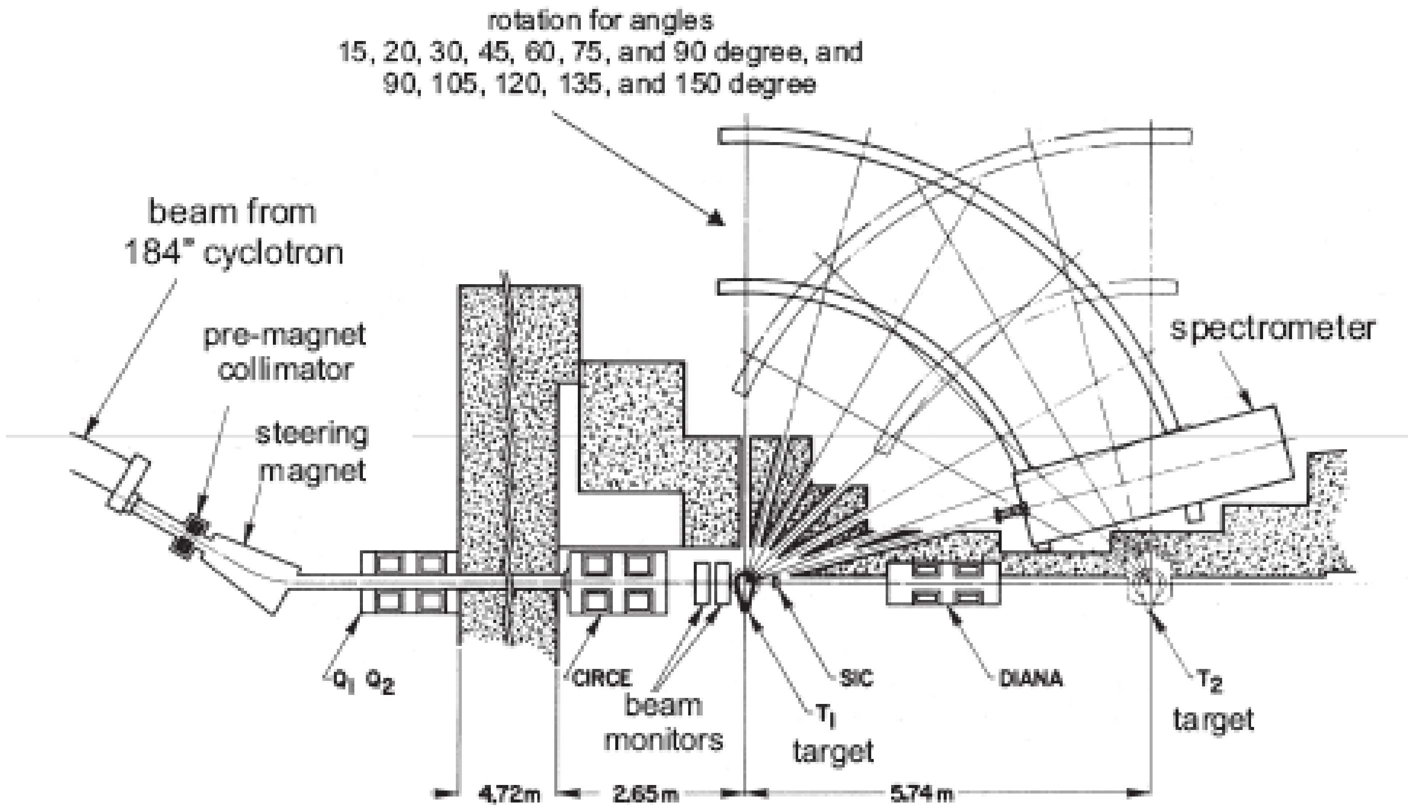

Sketch of the Cochran experiment at Berkley

(incident proton energy 730 MeV)

target material	density [g cm^{-2}]	target material	density [g cm^{-2}]
liquid H_2	density [a]	Cu	0.97
CD_2	1.13	Ag	1.08
Be	0.90	Ta	1.28
C	1.10	Pb	1.90
Al	0.97	Th	1.01
Ti	0.76		

a) The density for liquid H_2 is given in 1.59×10^{23} protons cm^{-2}

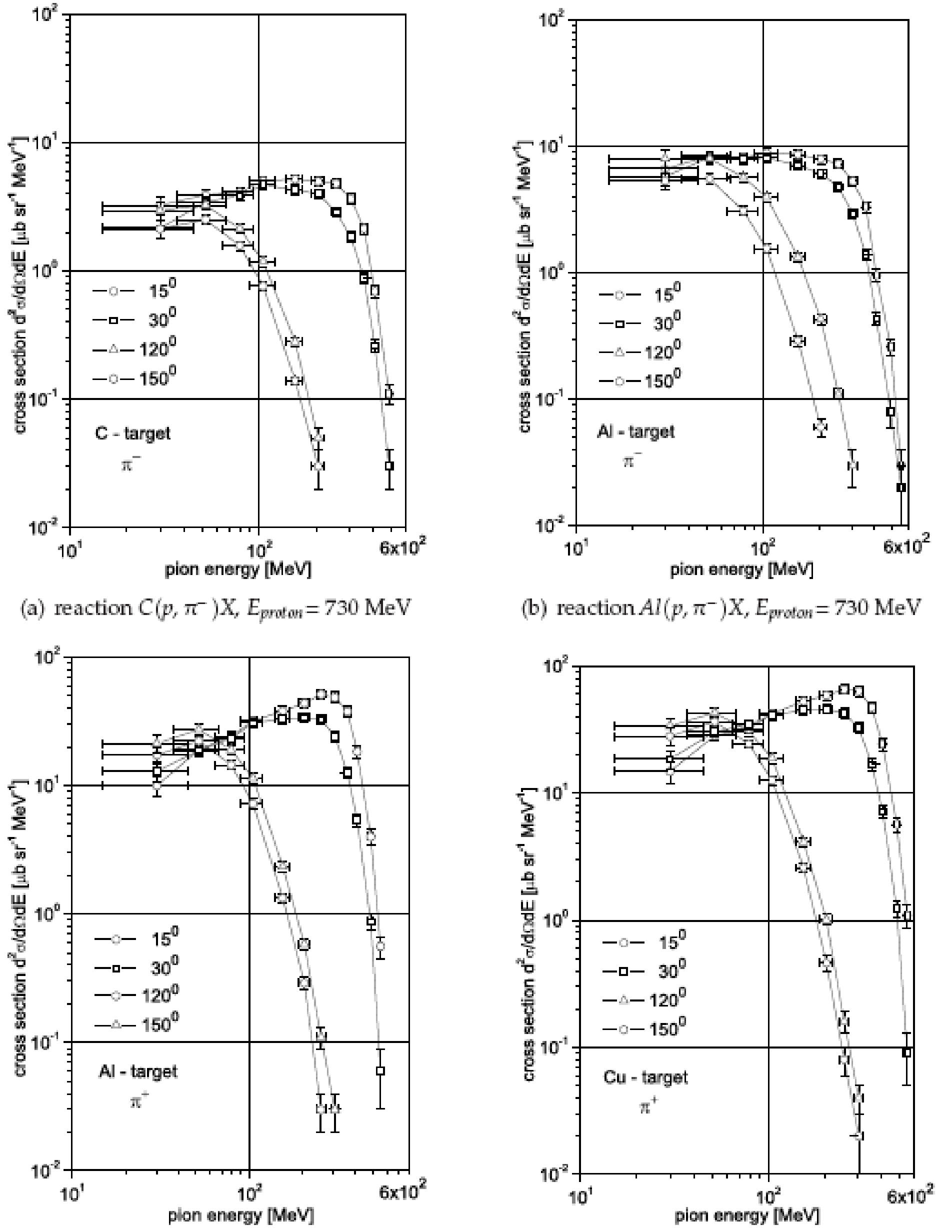

(a) reaction $C(p, \pi^-)X$, $E_{proton} = 730$ MeV

(b) reaction $Al(p, \pi^-)X$, $E_{proton} = 730$ MeV

(c) reaction $Al(p, \pi^+)X$, $E_{proton} = 730$ MeV

(d) reaction $Cu(p, \pi^+)X$, $E_{proton} = 730$ MeV

Fig. 10.30 Proton induced double differential $\pi^\pm$ production cross sections for C, Al, and Cu targets at scattering angles of 15^0, 30^0, 120^0, and 150^0 at an incident proton energy of 730 MeV. Data are from Ref. [124].

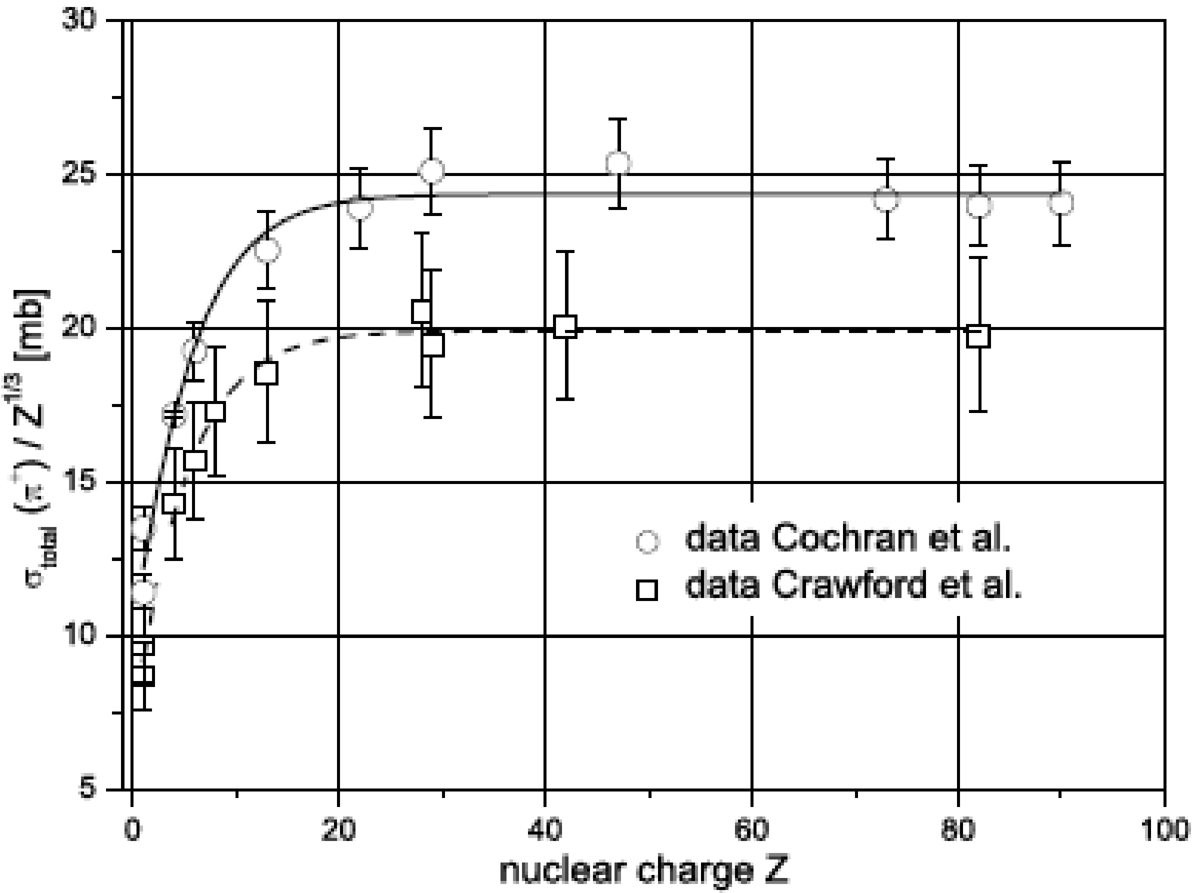

Total production for π⁺ from various targets divded by $Z^{1/3}$

(Cochran incident protons 730 MeV, and Crawford 585 MeV)